Journal of Pharmaceutical and Biomedical Analysis 50 (2009) 200–209

Contents lists available at ScienceDirect

Journal of Pharmaceutical and Biomedical Analysis

journal homepage: www.elsevier.com/locate/jpba

Biotransformation and in vitro assessment of metabolism-associated drug–drug interaction for CRx-102, a novel combination drug candidate

Zhi-Yi Zhang, Mei Chen, Jennifer Chen [1], Mahesh V. Padval, Vikram V. Kansra *

Department of Preclinical Development and Formulations, CombinatoRx Inc., 245 First St. 4th Floor, Cambridge, MA 02142, United States

ARTICLE INFO

Article history:
Received 23 February 2009
Received in revised form 9 April 2009
Accepted 10 April 2009
Available online 19 April 2009

Keywords:
Dipyridamole
Prednisolone
CYP3A4
Drug–drug interaction
Biotransformation
Combination drug

ABSTRACT

CRx-102 is an oral synergistic combination drug which contains the cardiovascular agent, dipyridamole (DP) and a very low dose of the glucocorticoid, prednisolone (PRED). CRx-102 works through a novel mechanism of action in which DP selectively amplifies the anti-inflammatory activity of PRED without replicating its side effects. CRx-102 is in clinical trials for the treatment of osteoarthritis. Here we delineate the in vitro metabolism and explore the potential for a drug–drug interaction between the active agents in CRx-102. Our study using human hepatocyte suspensions showed that both DP and PRED were metabolized by CYP3A4 isozymes, resulting in the formation of diverse arrays of both oxidative and oxidative-reduced metabolites. Within phase 1 biotransformation, CYP3A4 was one of the pathways responsible for the metabolism of PRED, while phase 2 biotransformation played a significant role in the metabolism of DP. Glucuronidation of DP was substantial and was catalyzed by many UGT members, specifically those in the UGT1A subfamily. Based on the tandem mass (MS/MS) product ion spectra (PIS) acquired, the major metabolites of both agents, namely, monooxygenated, mono-N-deethanolaminated, dehydrogenated and O-glucuronidated metabolites of DP and the monooxygenated (e.g., 6-hydroxyl), dehydrogenated (prednisone) and reduced (20-hydroxyl) metabolites of PRED, were identified and elucidated. The affinities for DP biotransformation, including CYP3A4-mediated oxidative pathways and UGT-mediated O-glucuronidation, appeared high (K_m < 10 μM), as compared with the modest affinities of PRED biotransformation catalyzed by CYP3A4 (K_m ~ 40–170 μM). DP, but not PRED, exerted a minimal inhibitory effect on the drug-metabolizing CYP isoforms, including CYP3A4, which was determined using a panel of CYP isoform-preferred substrate activities in pooled human liver microsomal (HLM) preparations and microsomal preparations containing the recombinant enzymes (K_i ~ 2–12 μM). Using the DP maximal plasma concentration (C_{max}) observed in the clinic and a predictive mathematical model for metabolism-associated drug–drug interaction (DDI), we have demonstrated that there is little likelihood of a pharmacokinetic interaction between the two active agents in CRx-102.

1. Introduction

CRx-102 is a synergistic combination drug candidate comprising a very low dose of the glucocorticoid, prednisolone (PRED) and the cardiovascular drug, dipyridamole (DP). The PRED contained in CRx-102 is at the low end of the recommended daily maintenance dose usually used to treat inflammatory conditions (2.5–15 mg) and is generally considered to be "sub-therapeutic." CRx-102 is thought to act through a novel mechanism of action in which DP selectively and synergistically enhances the anti-inflammatory and immuno-modulatory effects of PRED without amplifying the associated side effects [1]. This co-administration provides a combination approach to a dissociated glucocorticoid profile. A modified-release co-formulation with the aim of optimal co-exposure, with an improved tolerability profile, is being developed for each of the individual components of CRx-102.

Abbreviations: CAD, collision-associated dissociation; CE, collision energy; CYP, cytochrome P450; C_{max}, maximal plasma concentration; DEM, dextromethorphan; DIC, diclofenac; DP, dipyridamole; ESI, electrospray ionization; FURA, furafylline; HH, human hepatocytes; HLM, human liver microsomal preparations; HPLC, high-performance liquid chromatography; IS, internal standard; KETO, ketoconazole; MDZ, midazolam; MRM, multiple reaction monitoring; MS, mass spectrometry; MS/MS, triple quadrupole mass spectrometer; NADPH, β-nicotinamide adenine dinucleotide phosphate (reduced form); α-NF, α-naphthoflavone; PHEN, phenacetin; PI, product ion; PIS, product ion scan or product ion spectra; PRED, prednisolone; QUIN, quinidine; R_t, retention time; SIM, selective ion monitoring; S-MEPH, S-mephenytoin; TIC, total ion current; TICL, ticlopidine; TST, testosterone; UDPGA, uridine 5′-diphosphate glucuronic acid; UGT, UDP-glucuronosyltransferase.

* Corresponding author. Tel.: +1 617 301 7211; fax: +1 617 301 7109.
E-mail address: vkansra@combinatorx.com (V.V. Kansra).
[1] Current address: EPIX Pharmaceuticals Inc., 4 Maguire Rd., Lexington, MA 02421, United States.

0731-7085/$ – see front matter © 2009 Elsevier B.V. All rights reserved.
doi:10.1016/j.jpba.2009.04.013

Combination therapy has often proven to be more effective than monotherapies in the clinic, and is one of the current trends in medicine, especially in the treatment of chronic and life-threatening ailments, including arthritis, diabetes and cancer [2–4]. Understanding the metabolism and the associated interactions for combination drugs is more intricate compared to single agent. One reason why combination drugs may achieve superior therapeutic efficacy is because of a metabolic interaction between the active agents that enhances the pharmacokinetic (PK) profiles for each agent. Both DP and PRED are extensively metabolized by the cytochrome P450 enzymes (CYPs) in humans [5], known to be responsible for the phase 1 metabolism of the vast majority of therapeutic agents [6]. While being biotransformed mainly via glucuronidation (the most common human phase 2 conjugative pathway), DP metabolism has not been delineated with respect to the involvement of phase 1 enzymes in humans. In contrast, it is thought that phase 1 enzymes, especially CYP3A4, may play a role in PRED metabolism [7,8]. The responsible metabolic enzymes need further characterization, thereby warranting further investigation [9,10].

Expressed abundantly in human livers and intestinal epithelia, CYP3A4 exhibits a broad substrate spectrum, and is principally responsible for the metabolism of nearly half of all currently prescribed therapeutic agents [11,12]. The enzyme activity of members in the CYP3A subfamily elicit marked ethnic and inter-individual variability and their expression can be modulated by both endogenous and exogenous stimuli, thereby resulting in CYP3A4-associated drug–drug interaction (DDI), which is frequently observed in the clinic [13,14]. It is important to understand the metabolic pathways involved for each agent during the development of combination drugs, especially if the active agents are the substrates of CYP3A4.

Understanding the biotransformation of DP and PRED is essential for the evaluation of potential risk for DDI between PRED and DP in CRx-102. Using human liver microsomal (HLM) preparations, cDNA-expressed metabolic enzymes and primary human hepatocytes (HH), we investigated the biotransformation of the active agents in CRx-102. The investigation focused on the identification of the metabolites and metabolic enzymes and the interactions of these responsible enzymes. Based on the enzyme interactions (CYP3A4 inhibition, in particular) we predicted the potential impact on the clinical PK of these active agents and the other co-administered agents. Our results indicate that neither of the active agents in CRx-102 should show an interactive suppression of the metabolism of the other, nor do they affect the pharmacokinetics of potential concurrent drugs that are the substrates of CYP3A4.

2. Experimental

2.1. Chemicals

DP and PRED were obtained from Sigma–Aldrich Chemical Corp. (St. Louis, MO, USA). Acetaminophen, alamethicin, debrisoquine, dextromethorphan (DEM), dextrorphan, diclofenac (DIC), furafylline (FURA), 4-hydroxydiclofenac, 6β-hydroxytestosterone, ketoconazole (KETO), *S*-mephenytoin (S-MEPH), midazolam (MDZ), α-naphthoflavone (α-NF), phenacetin (PHEN), quinidine (QUIN), reduced β-nicotinamide adenine dinucleotide phosphate (NADPH), sulfaphenazole (SULF), testosterone (TST) ticlopidine (TICL), and uridine diphosphate glucuronic acid (UDPGA) were all obtained from Sigma–Aldrich Chemical Corp. (St. Louis, MO, USA). 4-Hydroxy-*S*-mephenytoin and 1′-hydroxymidazolam were purchased from Discovery Labware, BD Biosciences (Bedford, MA, USA). 20α- and 20β-hydroxyprednisolone were obtained from Steraloids (Newport, RI, USA). Methanol, acetonitrile, and formic acid were HPLC grade from Fisher Scientific USA (Pittsburgh, PA, USA).

2.2. Enzyme preparations and others

All enzyme sources, including the pooled HLM, the cDNA-expressed human enzymes and the cryopreserved HH were obtained from Discovery Labware, BD Biosciences (Bedford, MA, USA). The cDNA-expressed proteins included CYPs (CYP1A1, CYP1A2, CYP1B1, CYP2A6, CYP2B6, CYP2C8, CYP2C9, CYP2C19, CYP2D6, CYP2E1, CYP3A4, CYP3A5, and CYP4A11), and UDP-glucuronosyltransferases (UGT1A1, UGT1A3, UGT1A4, UGT1A6, UGT1A7, UGT1A8, UGT1A9, UGT1A10, UGT2B4, UGT2B7, UGT2B15, and UGT2B17). The controls were the microsomal preparations of the host cells without the expression of human enzymes. The inhibitory antibodies were CYP form-preferred. The donors of the cryopreserved hepatocytes, a 46-year-old female Caucasian and a 15-year-old male Caucasian, had no history of smoking or alcohol consumption and no record of liver impairment.

2.3. Metabolism and enzyme identification

Metabolism was determined based on the formation of the metabolites in the reaction mixtures compared to the respective controls. DP or PRED (5–200 μM) was incubated in the phosphate-buffered saline (PBS) reaction mixtures. The reaction mixtures (total volume of 200–500 μL) contained HLM (0.5–2 mg/mL of the proteins), recombinant CYPs (50 pmol/mL) and human hepatocytes (approximately 4×10^6 mL^{-1}). CYP inhibitors, including FURA (10 μM), α-NF (2 μM), SULF (10 μM), TICL (5 and 10 μM), QUIN (0–50 μM), KETO (0–50 μM), or inhibitory antibodies against CYP1A1, CYP2C8, CYP2D6 and CYP3A4 (as appropriate) were added in the enzyme reaction mixtures prior to incubation. The reaction was initiated upon the addition of the water solution of NADPH (approximately 1.2 mM) and the methanol solution of DP or PRED, and carried out at 37 °C for 20–120 min.

The metabolism by the recombinant UGTs was initiated with the addition of UDPGA (5 mM). The UGT reaction mixtures, besides the presence of alamethicin (200 μg/mL), were similar to those for the CYP reactions.

At the end of incubation, the reaction was stopped by quickly cooling the test tube on ice, followed by the addition of 100 μL or equal volume of methanol, containing an internal standard (IS) debrisoquine (1 μg/mL), if appropriate. The samples were centrifuged in a microcentrifuge at 16,000 × *g* for approximately 10 min, and the supernatant was transferred (after being filtered through a spin filter [0.22 μ], if appropriate) to a HPLC vial for LC/UV/MS or LC/MS/MS analyses.

2.4. CYP inhibition profiling and prediction of drug–drug interaction

The incubation mixtures (200 μL) contained HLM proteins (0.5 mg/mL), DP (0.1–100 μM), PRED (0.1–100 μM), CRx-102 (0.5 and 5 μM of PRED and 3 and 30 μM of DP, respectively), one of the CYP-form preferred probe substrates including PHEN (20 μM), DIC (2.5 μM), S-MEPH (40 μM), DEM (5 μM), MDZ (5 μM) or TST (50 μM), as well as NADPH (1.2 mM) in 100 mM sodium phosphate buffer (pH 7.4). The reaction was initiated upon the addition of DP or PRED with NADPH and incubated for 20 min in a 37 °C waterbath with gentle agitation. The reaction mixtures containing the probe substrates without DP or PRED were used as the full enzyme activity controls. Following incubation, the samples were prepared as described for LC/MS/MS analyses. The inhibitory effect, if detected,

was characterized by determination of the IC_{50} and K_i values, using ranges of concentrations (e.g., 0.1–50 μM of DP).

2.5. Instrumentation

LC/UV/MS and LC/MS/MS were applied for the study. Between two systems, LC/UV/MS was used mainly for DP determination and, occasionally, metabolite profiling; quantitative analyses and metabolite structural elucidation were mainly achieved upon the application of LC/MS/MS.

LC/UV/MS (Agilent, Palo Alto, CA, USA) was comprised of HPLC (Agilent 1100) including a quaternary pump, an autosampler, a degasser, a column compartment, a diode-array detector, and a single quadrupole mass spectrometer (MS). ChemStation (Version A. 09; Agilent, Palo Alto, CA, USA) was used to control the operation and acquire the data.

The metabolites were separated on a Zorbax Extend C18 column (150 mm × 4.6 mm, Agilent, Palo Alto, USA) at 35 °C. The mobile phase A was water with 0.1% (v/v) formic acid, and B was methanol with 0.1% (v/v) formic acid. The gradient (B) was 10% (0–1 min), 70% (11–16 min), and 10% (16 min and after). The flow rate was 500 μL/min. The MS was operated at positive electrospray ionization (ESI) with 4.0 kV ionization potential and 350 °C ion source temperature. Other parameters included 12 L/min drying gas flow, 45 psi nebulizer gas pressure, and 100 V fragmentor potential. Total ion current (TIC) and selected ion monitoring (SIM) were used during the operation. DP, monooxygenated, mono-, and bis-deethanolamine metabolites were detected at *m/z* 505, 521, 461, and 417, respectively, with UV absorbance at 254, 282, and 365 nm being recorded.

LC/MS/MS was comprised of HPLC (Agilent, Palo Alto, CA, USA) with a Cohesive leap autosampler (Cohesive Technologies, Franklin, MA, USA), and a triple quadruple mass spectrometer (SCIEX API3000; Applied Biosystems, Foster City, CA, USA). The HPLC system, besides the Cohesive autosampler, consisted of a column compartment, a degasser, and a binary pump. The metabolites of DP, PRED, and CYP probe substrates were separated on a Phenomenex Luna C18 (2) column (100 mm × 2.1 mm) with conventional mobile phase gradients at ambient temperature. The mobile phase A was water with 0.1% (v/v) formic acid, and B was methanol or acetonitrile with 0.1% (v/v) formic acid. The flow rate was 300 μL/min. In the biotransformation experiments employing the human hepatocytes, Waters Symmetry Shield RP18 column (100 mm × 2.1 mm) was applied with a typical gradient (B) of 5% (0–2 min), 30% (8 min), 95% (10–15 min), and 5% (15.5 min and after). The mobile phases were 5 mM ammonium acetate at pH 4.8 (A) and acetonitrile (B). Operations of the HPLC and the MS/MS were controlled using software Aria OS™ (Cohesive Technologies, Franklin, MA, USA) and Analyst (Version 1.4, Applied Biosystems), respectively, in a synchronized fashion. The MS/MS was operated at positive ESI with 5 kV of ionization potential and 350–400 °C of ion source temperature. Nebulizing, curtain, and collision-associated dissociation (CAD) gas were typically 8, 12, and 10, respectively. Multiple reaction monitoring (MRM) and product ion scans (PIS) were employed with the MS/MS conditions, i.e., collision energies (CE), being adjusted accordingly. In MRM application, the transition ions (*m/z*) for the detection of DP and PRED were 505 → 429 and 361 → 147, respectively. The MRM transitions (*m/z*) used in the quantification of CYP probe substrate activities were listed as follows: 152 → 110 (acetaminophen), 312 → 231 (4′-hydroxydiclofenac), 235 → 150

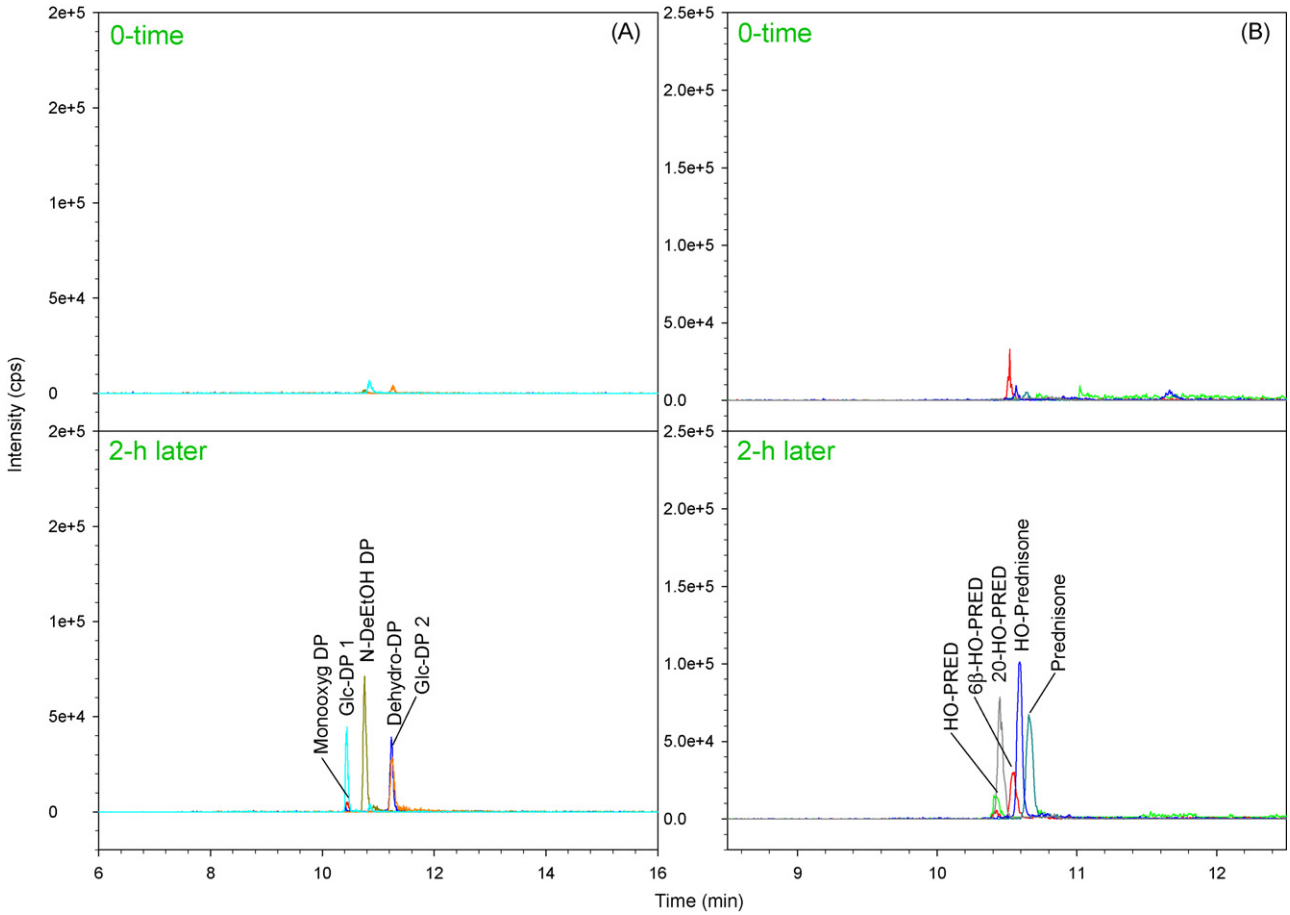

Fig. 1. Metabolic profiles of DP (A) and PRED (B) determined in the suspension of cryopreserved human hepatocytes. The metabolic profiles shown as the metabolite-specific MRM chromatograms were qualitative. The other experimental conditions were described in Section 2.

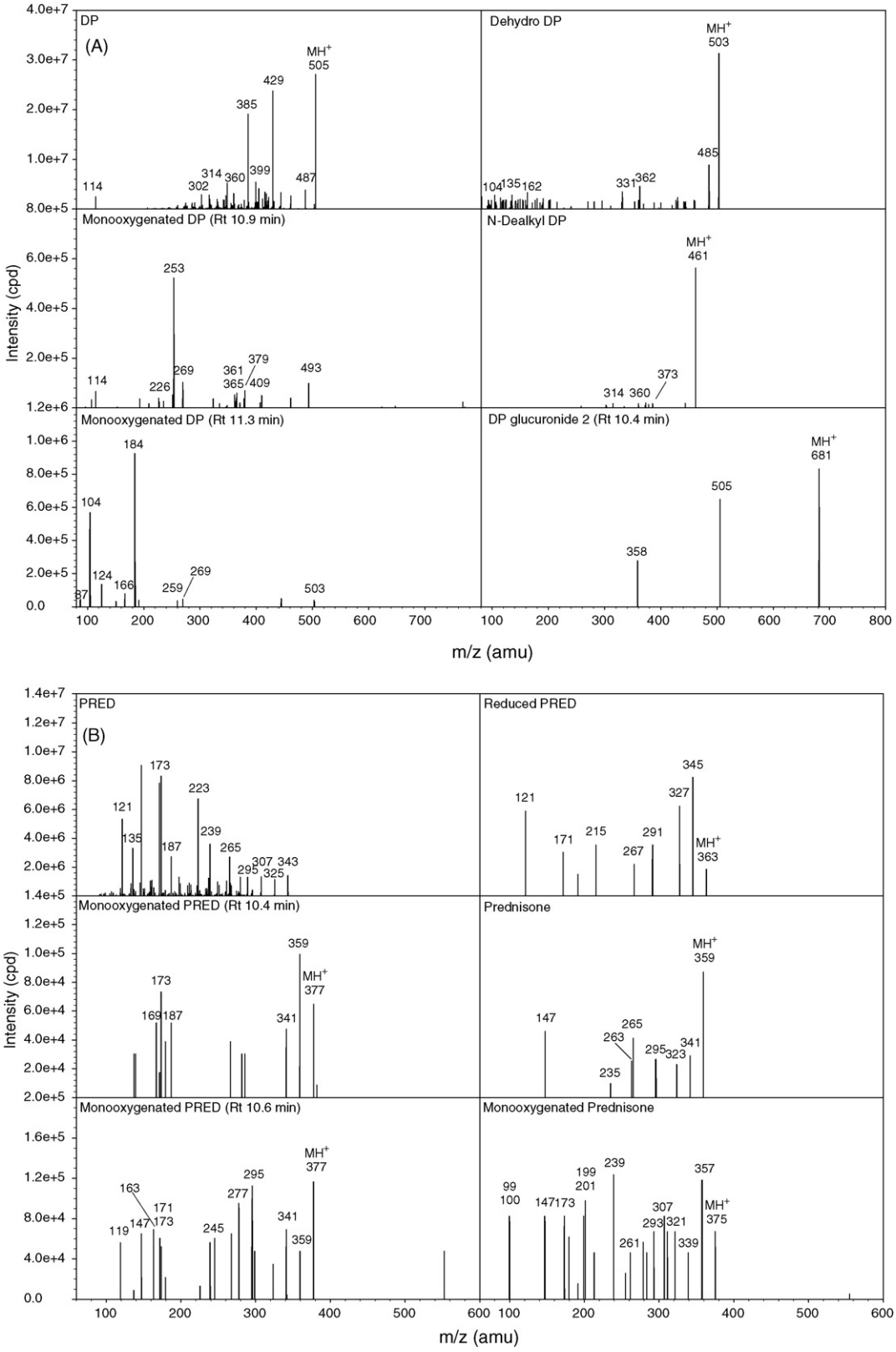

Fig. 2. MS/MS product ion spectra of DP (A) and PRED (B) and their major metabolites formed in the suspension of cryopreserved human hepatocytes. The collision energies for generating product ions were higher for DP and its metabolites (40–60 eV) than what used for PRED and its metabolites (20–30 eV). The other instrumental conditions were described in Section 2.

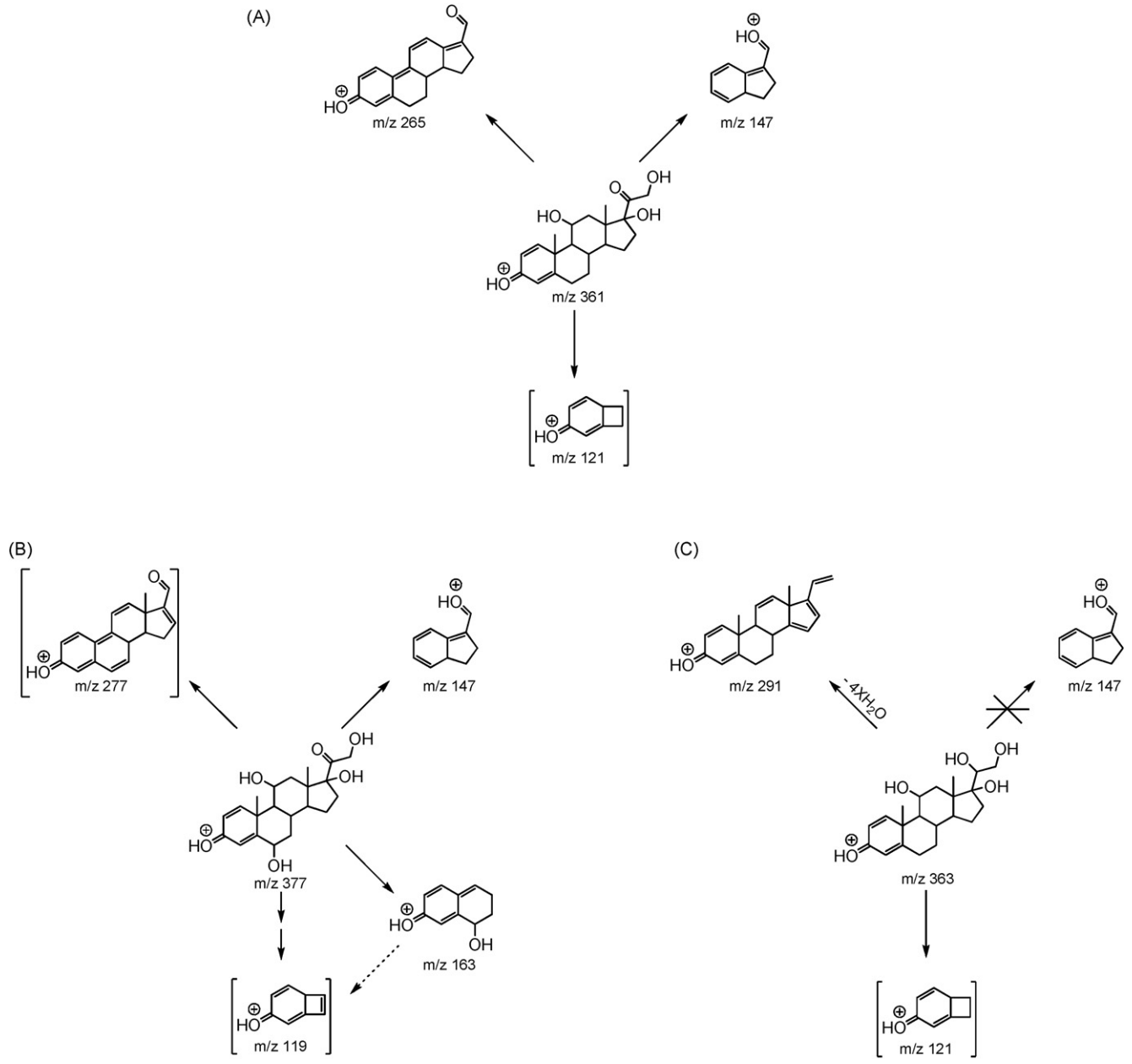

Fig. 3. Proposed diagnostic MS/MS product ions for PRED (A), 6β-HO- (B) and 20-HO-PRED (C). Diagnostic ions were based on the MS/MS PIS and proposed ion fragmentation of PRED quasi-molecular ions.

(4′-hydroxymephenytoin), 258 → 157 (dextrorphan), 342 → 324 (1′-hydroxymidazolam), 305 → 287 (6β-hydroxytestosterone), and 176 → 124 (debrisoquine).

2.6. Data analysis

Calibration curves were generated using a series of diluted stock solutions of compound standards prepared in a manner similar to that for the reaction samples described. Replicates were always determined for quantification based on peak area ratios of metabolites over the respective IS against the respective concentrations of the metabolites. Values relative to the corresponding controls were presented if the synthetic references were unavailable. Metabolic rates were determined using GraphPad Prism (Version 3.02; San Diego, CA, USA) or SigmaPlot (Version 11.00, SPSS Inc., Chicago, IL, USA). Enzyme kinetic parameters, such as K_m, IC_{50}, and K_i, were determined primarily upon the nonlinear regression analyses [15].

The key equations (Eq.) employed in the study are shown as follows:

$$\text{risk index}: \quad \text{RI} = \frac{C_{max}}{K_i} \tag{1}$$

$$\text{pharmacokinetic alteration}: \quad \frac{\text{AUC}_i}{\text{AUC}} = \frac{K_i + I}{K_i + I(1 - f_m f_{m,i})} \tag{2}$$

where C_{max} is maximum drug (inhibitor) concentration detected in circulation. K_i is inhibition constant. f_m and $f_{m,i}$ are the fraction of drug clearance by total responsible CYP members and the fraction of drug clearance by the inhibited CYP member(s) in total responsible CYP members, respectively. Eq. (2) was derived from the previously published equation for accurate DDI prediction [16].

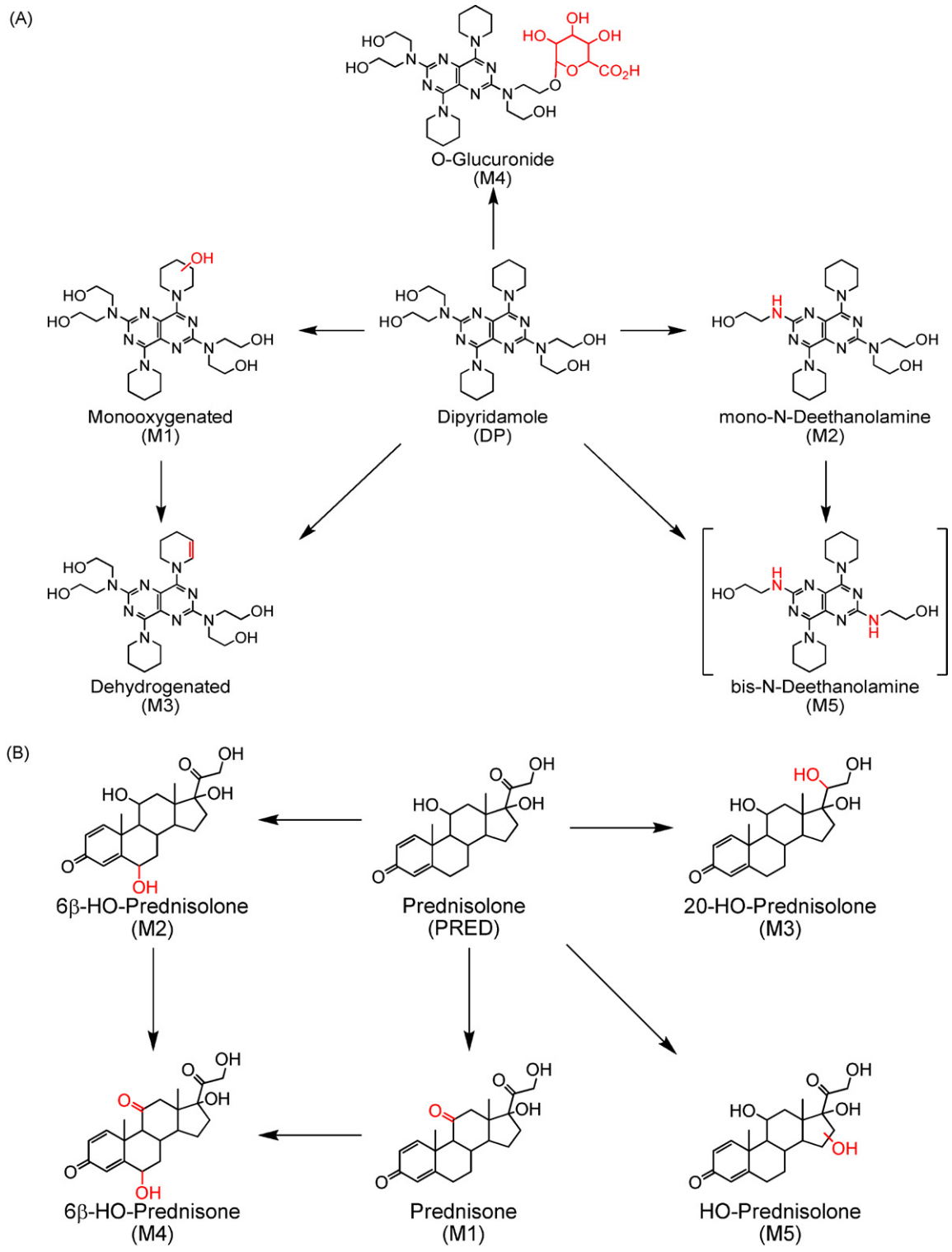

Fig. 4. Proposed hepatic DP (A) and PRED (B) biotransformation in humans. Markush structures are shown for the monooxygenated metabolites formed upon the hydroxylation of DP piperidinyl moieties (M1) and some of the fused rings of PRED (M5). The structural assignments of dehydro (M3) and bis-N-deethanolamine DP metabolites (M5) shown were speculative.

3. Results and discussion

3.1. Metabolite identification

While the metabolic profiles were initially studied using the pooled HLM and the recombinant CYP enzymes, they were finally determined in the suspensions of the cryopreserved primary HH. In HLM, DP and PRED were converted, in a time- and NADPH-dependent manner, to several phase 1 metabolites such as the monooxygenated DP and PRED metabolites, gauged upon the metabolite formation against the controls (i.e., the non-reaction or 0-time reaction mixtures, or the reaction mixtures that did not contain NADPH). The formation of phase 1 metabolites appeared to be extensive for PRED, but was somewhat limited for DP, suggesting

different roles for CYPs in DP and PRED metabolism. However, the metabolic profile of DP in HH became diverse, resulting from the substantial glucuronidation that did not require the supplement of exogenous UDPGA (Fig. 1).

The metabolites of DP and PRED were structurally elucidated based on the MS/MS spectral analyses. As shown in Fig. 2A, DP was efficiently ionized (*m*/*z* 505) and dissociated to a few product ions (e.g., *m*/*z* 429, 385, and 114) under relatively high CE (50–60 eV). Due to the concurrent multiple nitrogen atoms, the nitrogen rule was applicable in interpreting the product ions of DP and the metabolites, notwithstanding the limited diagnostic product ions [17]. The protonated molecular ions at *m*/*z* 521 (at minimum, two), 503, 461, and 681, detected in the hepatocyte suspensions after the incubation, were consistent with the monooxygenated, dehydrogenated, N-dealkylated, and glucuronyl-conjugated metabolites (likely two), respectively. The PIS exhibited by these putative metabolites was also supportive, for the relatively abundant dehydro-, dealkyl-, and glucuronide metabolites, in particular. For instance, the protonated ion of a smaller metabolite (M2) at *m*/*z* 461, possessing an even number (eight) of nitrogen atoms as DP (the nitrogen rule), appeared in a large agreement with a loss of N-ethanolamine (−44 amu). The large product ions (PIs) at *m*/*z* 314 and 360 were seen for both DP and this metabolite, further confirming their common core moieties. Moreover, one of the putative glucuronides (+176 amu) was ionized and dissociated to just two PIs (*m*/*z* 505 and 358). These ions indicated that PI at *m*/*z* 505 was the protonated DP, resulting from the loss of dehydroglucuronic acid, due to the weak glycosidic bond, whereas the PI at *m*/*z* 358 was the dehydrogenated counterpart of the PI of DP at *m*/*z* 360. While not being specific to the site of glucuronidation, the formation of glucuronide metabolites by human hepatocytes was evident, and the major glucuronide (M4) would be speculated as an O-glucuronide because of the steric hindrance for the formation of quaternary ammonium glucuronide. The formation of an N-glucuronide should not be completely ruled out, as more than one glucuronide metabolite might be formed by these human cells (Fig. 1).

In humans, it has been suggested that DP undergoes enterohepatic circulation [18,19], a well-known interplay between the hepatic glucuronidation and the intestinal elimination/reabsorption. While CYP3A4-mediated oxidative metabolism likely plays a role in the metabolism of DP, the simultaneous glucuronidation of DP, which competes with the oxidative pathways, has been demonstrated to be the more prevalent mechanism in DP clearance [18,20].

The MS/MS spectral results were, in general, structurally revealing for PRED and the primary metabolites (Fig. 2B), because of the diagnostic PRED product ions at *m*/*z* 121, 147, and 265 (Fig. 3A). Therefore, the hydroxylated PRED (M2) displaying PIs at *m*/*z* 119 and 163 is consistent with one of the major hydroxyl metabolites, 6β-HO-PRED (Fig. 3B) [21]. Similarly, the detection of prednisone M1, a well-known PRED metabolite, was conceivable; beyond the 2-amu deficiency of the quasi-molecular ions, the indicator of dehydrogenation, the product ion at *m*/*z* 263, in addition to one at *m*/*z* 265, could result from the substitution of a hydroxyl group with a carbonyl group on the fused ring system. Meanwhile, two hydroxyl groups were retained in this metabolite because of the H_2O-loss PIs (*m*/*z* 341 and 323), compared to three hydroxyl groups possessed by PRED (*m*/*z* 343, 325, and 307) (Fig. 2B). One of the quasi-molecular ions of PRED metabolites formed by HH at *m*/*z* 363 (M3) was a reduced (or hydrogenated) product because of the 2-amu increment, compared to PRED (MH^+ *m*/*z* 361). This metabolite was assigned to be 20-HO-PRED. The PI at *m*/*z* 291, resulting from the neutral losses of 72 amu, or four H_2O molecules formed from the hydroxyl groups dissociated under a low CE (20 eV), would not arise unless one of the carbonyl residues was reduced to a hydroxyl group. The abundant PI at 121, as seen for PRED, suggested the intact C3 or the ring carbonyl group and thus, the reduction on the

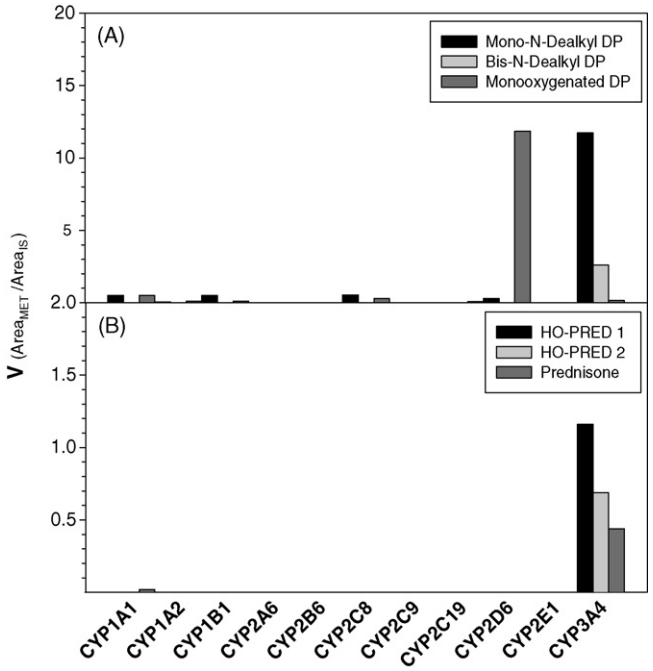

Fig. 5. Metabolite formation of DP (A) and PRED (B) by cDNA-expressed CYP forms. The activities shown were the mean of duplicate measurements. The other assay conditions were depicted in Section 2.

C20 carbonyl group (Fig. 3C). This assignment was confirmed by a comparison to the optically pure reference standards (20α- and 20β-HO-PRED), since identical HPLC retention time (R_t) and MS/MS PIS were recorded for the references and the metabolite (data not shown). Phase 2 biotransformation was not seen for PRED in suspensions of human hepatocytes. Unlike most steroids, PRED is not a substrate for UDP-glucuronosyltransferases, although it possesses the potential conjugative sites (i.e., 17-OH and 3-OH [potentially existing due to the enol-keto tautomerization]) [22,23]. Thus, the structural variation may have a marked impact on the metabolic pathways of steroids. The metabolic pathways of PRED we detected in HH appeared consistent with those reported previously based on metabolites found in urine from patients after PRED administration [21,24]. The consistency between the metabolic profiles seen in the clinic and those generated in HH confirms the central role of the liver metabolism in the elimination of PRED. Therefore, the metabolic profiles of DP and PRED in human livers were proposed (Fig. 4).

3.2. Responsible enzyme identification

The enzymes responsible for the major pathways were kinetically delineated in HLM containing the recombinant proteins, using the chemical inhibitors and inhibitory antibodies.

As shown in Fig. 5A, three DP phase 1 metabolites, namely the mono- and bis-N-deethanolamine and the major hydroxylated metabolites, were evaluated for their formation by the individually expressed drug-metabolizing CYP members in the presence of NADPH. CYP3A4 and CYP2D6 exhibited relatively higher capacities to form DP metabolites, with lower activities shown by CYP1A1, CYP1B1, and CYP2C8. Among the CYP-form preferred inhibitors tested, the rates of DP metabolite formation were only affected by ketoconazole, a CYP3A4 inhibitor, in a concentration-dependent fashion, with the formation of N-deethanolamine metabolites being most markedly affected (Fig. 6). Similar inhibitory effects were seen with the anti-CYP3A4 antibodies. Meanwhile, the anti-CYP2D6 antibodies, at higher concentrations also inhibited the

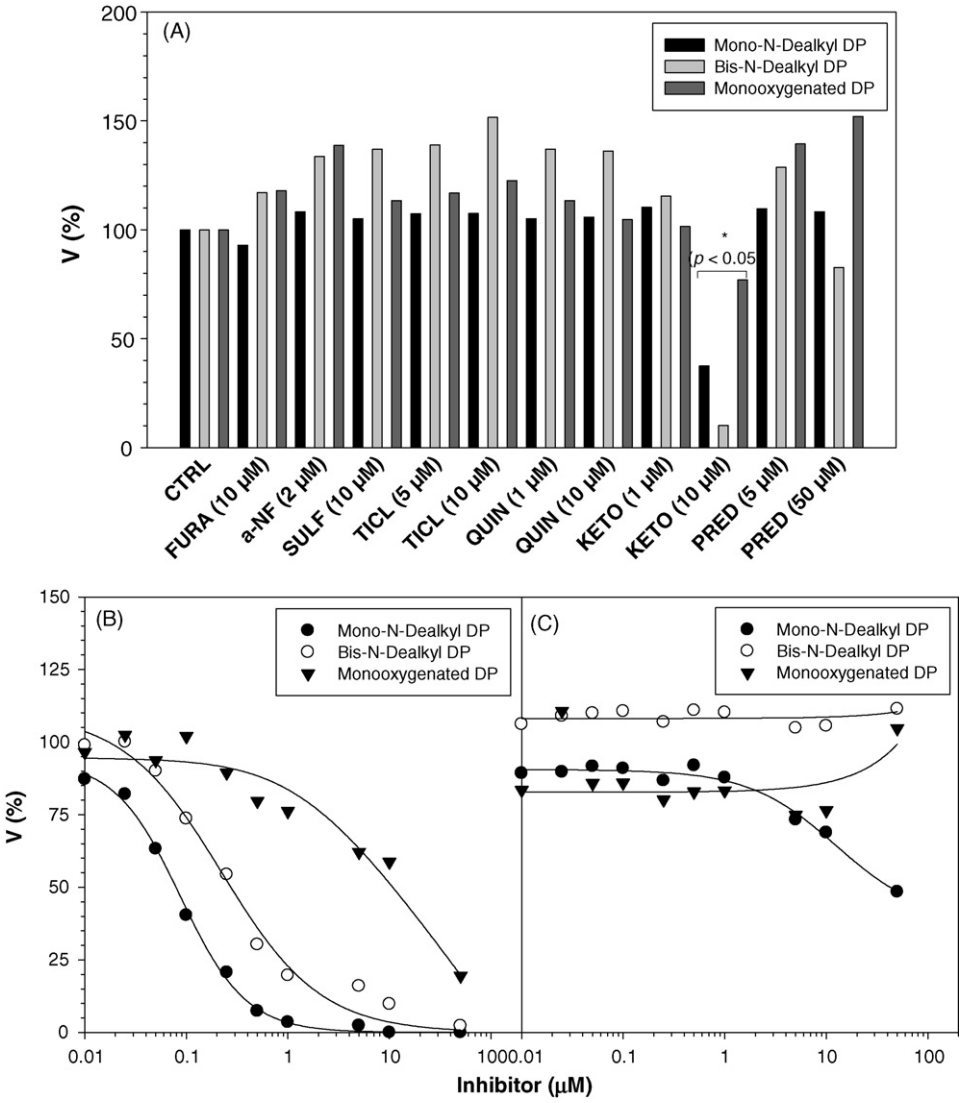

Fig. 6. Effect of chemical inhibitors and PRED on the activities of DP metabolite formation in HLM. Effect of CYP-form preferred chemical inhibitors and PRED on the NADPH-dependent formation of DP metabolites (A). Concentration-dependent suppression on DP metabolite formation by ketoconazole (B) and quinidine (C). The activities shown were the mean of duplicate measurements. The other assay details were described in Section 2.

formation of DP metabolites, but to a lesser extent (data not shown). Thus, although a metabolic role was demonstrated for CYP2D6 in the formation of a monooxygenated metabolite (Fig. 5A), CYP3A4 is responsible for the primary DP oxidative biotransformation.

In a preliminary study, multiple forms of UGTs were considered to be contributing to DP glucuronidation. A large panel of cDNA-expressed human UGT members were probed with DP (5 μM). Many UGT enzymes, including UGT1A1, 1A3, 1A4, 1A8, 1A9, and 2B7, exhibited relatively high turnover capacities towards the formation of DP glucuronide. Moreover, DP glucuronidation, mediated by the individual UGTs (1A1, 1A3, and 1A4) and HLM, was consistently of high affinity (K_m < 10 μM) (Table 1).

CYP3A4 was principally, if not solely, responsible for PRED metabolism (Fig. 5B). The minor involvement of CYP1A1 in PRED metabolism appears irrelevant, not only because of the negligible turnover rate (Fig. 5B), but also due to the diminished, extrahepatic expression [25]. The apparent values of K_m for CYP3A4-mediated DP and PRED metabolism were determined (Table 1). Interestingly, in contrast to the consistent high affinity DP glucuronidation mediated by HLM and individual UGT members, the affinity of oxidative DP metabolism in HLM appeared variable. However, such a variation appeared consistent with an approximately 10-fold difference in K_m detected in the reactions catalyzed by the recombinant CYP3A4 and CYP2D6. CYP3A4-mediated high affinity reactions had an apparent average K_m value of 5 μM and CYP2D6-mediated low affinity reactions had an average K_m value around 45 μM. The apparent K_m values for PRED biotransformation-mediated by HLM

Table 1
Apparent K_m of CYP- and UGT-catalyzed dipyridamole and prednisolone biotransformation.

Enzymes	K_m (μM)[a]		
	DP		PRED
	Phase 1 pathways	Phase 2 pathway (glucuronidation)	Phase 1 pathways
HLM	4–42	3	60–97
CYP3A4	2–8		40–166
CYP2D6	42–47		
UGT1A1		2	
UGT1A3		1	
UGT1A4		7	

[a] Estimated based on the nonlinear regression analyses of multiple pathways.

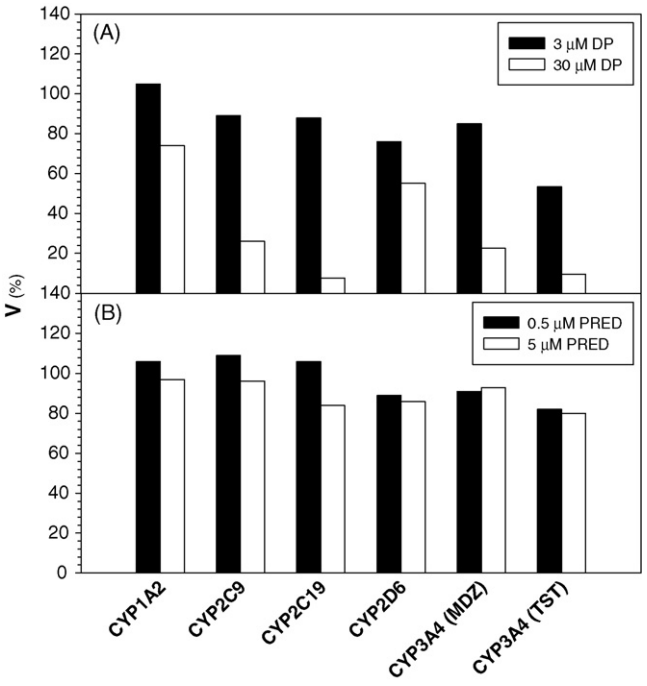

Fig. 7. Effect of DP (A) and PRED (B) on the activities of cDNA-expressed drug-metabolizing CYP members. The activities shown were the mean of duplicate measurements. The assay procedures and conditions for the CYP substrate assays were depicted in Section 2.

and CYP3A4, were comparable and consistent with the predominant role of CYP3A4 in PRED metabolism.

3.3. Characterization of CYP inhibition and risk prediction for drug–drug interaction

Applying the enzyme-preferred substrate activities, we estimated the inhibitory profiles for the major drug-metabolizing CYP enzymes at pharmacologically relevant concentrations (approximately 1× and 10×), specifically 0.5 μM and 5 μM PRED, and 3 μM and 30 μM DP, based on the C_{max} detected in the clinic [25–28] (Fig. 7). PRED had little effect at these concentrations. In contrast, DP suppressed the activities of several CYP members, including CYP2C9, CYP2C19, CYP2D6, and CYP3A4 in a concentration-dependent manner, with the effects on CYP2C19 and CYP3A4 being most evident. Consistently, the inhibition constants (K_i) were determined in the low micromolar range, especially for CYP3A4 and CYP2C19 (Table 2). With a onefold variation gauged using two substrate probes, midazolam and testosterone, the apparent K_i values for CYP3A4 inhibition appeared representative, given the well-known potential for atypical kinetics of CYP3A4-catalyzed reactions [29].

The prediction of DDI risk due to the enzyme inhibition by DP was initially undertaken by applying the risk index (RI; Eq. (1)). On average, RI was calculated to be 0.8 for CYP3A4 inhibition when C_{max} of 3 μM was adopted, indicating a potential risk for DDI. Therefore, the impact on clinical PK, in particular the change of AUC, was quantitatively estimated using Eq. (2) ($AUC_i/AUC = (K_i + I)/[K_i + I(1 - f_m f_{m,i})]$), in which the fraction of drug clearance by total metabolic CYPs or f_m, and the fraction of dose metabolized by inhibited CYPs or $f_{m,i}$ are critical. While both CYP1A1 and CYP3A4 exhibited turnover capacities, CYP3A4 appeared primarily responsible for PRED phase 1 metabolism. CYP1A1 and possibly the metabolic CYP enzymes other than CYP3A4 likely play a very limited role in PRED metabolism because of the minimal level of hepatic expression, i.e., at least one order of magnitude lower hepatic expression [11], and the minimal catalytic capacities of CYP1A1 as compared to CYP3A4. Thus, $f_{m,i}$ was assumed to be 90%, a reasonable, although somewhat arbitrary assumption. Similarly, conjugative biotransformation was neither known for PRED nor detected in the suspension of primary hepatocytes in this study. Therefore, the conjugative pathway, if any, would be highly limited for PRED. Therefore, f_m for the overall CYP-mediated PRED metabolism would be predominant and presumed around 90% of the total metabolic clearance. Incorporated C_{max} of 2.7 μM following p.o. doses of 100 mg (QD) seen in clinic [26, in-house data], AUC_i/AUC was computed to be 1.6. Thus, the PK alteration is predicted to be, at most, moderate and thus clinically irrelevant [30].

Table 2
Inhibitory parameters for CYP inhibition by DP in pooled HLM.

Enzyme	Activity	Parameters (μM)	
		IC50[a]	K_i
CYP2C9	DIC-4′-OH	16.5	8.2
CYP2C19	S-MEPH-4-OH	3.5	1.7
CYP2D6	DEM-DeMe	24.0	12.0
CYP3A4	MDZ 1′-OH	10.0	5.0
	TST 6β-OH	4.9	2.4

[a] Mean ($N = 2$).

C_{max}/K_i or RI, a ratio without factoring in metabolic pathways and protein binding, is potentially deceiving because of the high protein binding (~98%) [31] and the involvement of multiple metabolic pathways, such as the predominant glucuronidation [18,20]. CYP3A4-mediated oxidation and UGT-mediated glucuronidation occur simultaneously and take place competitively in DP metabolism. Notwithstanding, we demonstrated a minimal risk of CYP3A4 inhibition by DP in altering the PK of PRED in the clinical setting (less than 1-fold increase in AUC) [30]. It is worth noting that such a negligible PK effect was predicted without taking the high DP protein binding into account, which would further alleviate the impact on the PK of PRED.

The potential for DDI resulting from the competition for the UGTs among the drug substrates has been also evaluated, since the major pathway of DP was glucuronidation. Neither UGT1A inhibitors, nor PRED were found to suppress DP glucuronidation in HLM (data not shown). This observation is consistent with the lack of association between UGT inhibition and DDI in clinic [32]. Multiple UGT enzymes, including at least five UGT1A subfamily members detected in this study, are apparently responsible for the glucuronidation with comparable affinities ($K_m \sim 1$–7 μM). DP, like the majority of the other UGT substrates [33], was not as selective for its conjugating enzymes, consistent with the attenuated impact on a given UGT member and the minimal potential for UGT-associated DDI.

4. Conclusion

In summary, we investigated the metabolism of prednisolone and dipyridamole, the active agents in the combination drug CRx-102. Prednisolone was converted by CYP3A4 to a series of phase 1 metabolites, while dipyridamole was metabolized by both CYPs (CYP3A4 and CYP2D6) and by UGT1A enzymes to phase 1 and glucuronide metabolites, respectively. The metabolites were structurally elucidated based on the MS/MS product ion spectra. In contrast to prednisolone, dipyridamole was delineated to be a weak inhibitor of CYP3A4, CYP2D6, and CYP2C. However, the suppression of these CYP enzymes, CYP3A4 in particular, did not appear clinically relevant from a drug–drug interaction perspective, because of the weak inhibitory potencies, the simultaneous UGT-mediated

metabolism, and high protein binding. Therefore, the present study indicates that neither active agent in CRx-102 would likely bear a risk for inhibiting the metabolism of the other, or the metabolism of concomitantly administered drugs, which are metabolized by drug-metabolizing CYP enzymes.

Acknowledgements

We would like to express our gratitude to John Newton and Karen D'Amour for their assistance in preparing this manuscript for publication and Camille P. Granvil for his scientific input.

References

[1] G.R. Zimmermann, W. Avery, A.L. Finelli, M. Farwell, C.C. Fraser, A.A. Borisy, Arthritis Res. Ther. 11 (2009) R12.
[2] E.W. St. Clair, Curr. Rheumatol. Rep. 1 (1999) 149–156.
[3] T. Hideshima, N. Raje, P.G. Richardson, K.C. Anderson, Ther. Clin. Risk Manage. 4 (2008) 129–136.
[4] H. Xiao, C.S. Yang, Int. J. Cancer 123 (2008) 983–990.
[5] A.E. Stuck, B.M. Frey, F.J. Frey, Clin. Pharmacol. Ther. 43 (1988) 354–362.
[6] F.P. Guengerich, Chem. Res. Toxicol. 21 (2008) 70–83.
[7] K.H. Lee, J.G. Shin, W.S. Chong, S. Kim, J.S. Lee, I.J. Jang, S.G. Shin, Eur. J. Clin. Pharmacol. 45 (1993) 287–289.
[8] H. Bergrem, O.K. Refvem, Proc. Eur. Dial. Transplant. Assoc. 19 (1983) 552–557.
[9] S.W. Carson, K.J. Letrent, M. Kotlyar, G. Foose, M.E. Tancer, Pharmacotherapy 24 (2004) 482–487.
[10] S.K. Yamashita, E.A. Ludwig, E. Middleton Jr., W.J. Jusko, Clin. Pharmacol. Ther. 49 (1991) 558–570.
[11] T. Shimada, H. Yamazaki, M. Mimura, Y. Inui, F.P. Guengerich, J. Pharmacol. Exp. Ther. 270 (1994) 414–423.
[12] J.C. Kolars, P. Schmiedlin-Ren, J.D. Schuetz, C. Fang, P.B. Watkins, J. Clin. Invest. 90 (1992) 1871–1878.
[13] R.P. Riechelmann, E.D. Saad, Cancer Invest. 24 (2006) 704–712.
[14] C.D. Scripture, A. Sparreboom, W.D. Figg, Lancet Oncol. 6 (2005) 780–789.
[15] P.C. Engel (Ed.), Enzymology Labfax, BIOS Scientific Publishers Limited, Oxford, 1996.
[16] K. Ito, T. Iwatsubo, S. Kanamitsu, K. Ueda, H. Suzuki, Y. Sugiyama, Pharmacol. Rev. 50 (1998) 387–412.
[17] Z.Y. Zhang, B.M. King, N.N. Mollova, Y.N. Wong, Drug Metab. Dispos. 30 (2002) 805–813.
[18] F. Nielsen-Kudsk, A.K. Pedersen, Acta Pharmacol. Toxicol. (Copenh). 44 (1979) 391–399.
[19] B. Terhaag, F. Donath, G. Le Petit, K. Feller, Int. J. Clin. Pharmacol. Ther. Toxicol. 24 (1986) 298–302.
[20] G. Breisenherz, F.W. Koss, A. Schuele, I. Gebauer, R. Baerisch, Froede, Arzneimittelforschungr 10 (1960) 307–312.
[21] V. Garg, W.J. Jusko, J. Chromatogr. 567 (1991) 39–47.
[22] J.M. Kjeld, J.M. Wieland, M. Puah, Clin. Chim. Acta 102 (1980) 119–126.
[23] J. Lépine, O. Bernard, M. Plante, B. Têtu, G. Pelletier, F. Labrie, A. Bélanger, C. Guillemette, J. Clin. Endocrinol. Metab. 89 (2004) 5222–5232.
[24] A. Vermeulen, E. Caspe, J. Biol. Chem. 234 (1959) 2295–2297.
[25] X. Ding, L.S. Kaminsky, Annu. Rev. Pharmacol. Toxicol. 43 (2003) 149–173.
[26] A. Dresse, C. Chevolet, D. Delapierre, H. Masset, H. Weisenberger, G. Bozler, G. Heinzel, Eur. J. Clin. Pharmacol. 23 (1982) 229–234.
[27] M. De Silva, B.L. Hazleman, J. Chakraborty, J. English, V. Marks, Clin. Rheumatol. 2 (1983) 299–302.
[28] S. Rohatagi, J. Barth, H. Möllmann, G. Hochhaus, A. Soldner, C. Möllmann, H. Derendorf, J. Clin. Pharmacol. 37 (1997) 916–925.
[29] T.S. Tracy, Curr. Drug Metab. 4 (2003) 341–346.
[30] H. Zhang, M.W. Sinz, A.D. Rodrigues, in: D. Zhang, M. Zhu, W.G. Humphreys (Eds.), Metabolism-Mediated Drug–Drug Interactions in Drug Metabolism in Drug Design and Development, John Wiley & Sons Inc., Hoboken, NJ, 2008.
[31] T.R. MacGregor, E.D. Sardi, J. Pharm. Sci. 80 (1991) 119–120.
[32] T.K. Kiang, M.H. Ensom, T.K. Chang, Pharmacol. Ther. 106 (2005) 97–132.
[33] T.B. Joseph, S.W. Wang, X. Liu, K.H. Kulkarni, J. Wang, H. Xu, M. Hu, Mol. Pharm. 4 (2007) 883–894.